Current Applied Physics 17 (2017) 222–229

Contents lists available at ScienceDirect

Current Applied Physics

journal homepage: www.elsevier.com/locate/cap

Engineered omnidirectional antireflection ITO nanorod films with super hydrophobic surface via glancing-angle ion-assisted electron-beam evaporation deposition

P. Nuchuay [a], T. Chaikeeree [a], M. Horprathum [b, *], N. Mungkung [c, **], N. Kasayapanand [a], C. Oros [d], S. Limwichean [b], N. Nuntawong [b], C. Chananonnawathorn [b], V. Patthanasettakul [b], P. Muthitamongkol [e], B. Samransuksamer [f], S. Denchitcharoen [f], A. Klamchuen [g], C. Thanachayanont [e], P. Eiamchai [b]

[a] School of Energy, Environment and Materials, King Mongkut's University of Technology Thonburi, Bangkok 10140, Thailand
[b] National Electronics and Computer Technology Center, National Science and Technology Development Agency, Pathum Thani 12120, Thailand
[c] Department of Electrical Technology Education, Faculty of Industrial Education and Technology, King Mongkut's University of Technology Thonburi, Bangkok 10140, Thailand
[d] Faculty of Liberal-arts, Rajamangala University of Technology Rattanakosin, Nakornpathom 73170, Thailand
[e] National Metal and Materials Technology Center, National Science and Technology Development Agency, Pathum Thani 12120, Thailand
[f] Department of Physics, Faculty of Science, King Mongkut's University of Technology Thonburi, Bangkok 10140, Thailand
[g] National Nanotechnology Center, National Science and Technology Development Agency, Pathum Thani 12120, Thailand

ARTICLE INFO

Article history:
Received 31 August 2016
Received in revised form
20 October 2016
Accepted 20 November 2016
Available online 22 November 2016

Keywords:
ITO nanorods
Glancing angle deposition
Transparent conductive oxide
Omnidirectional anti-reflection
Ion assisted electron beam evaporation

ABSTRACT

Growths of the indium tin oxide (ITO) nanorod films have been demonstrated by ion-assisted electron-beam evaporation with the glancing-angle deposition technique based on variation in deposition rate. Investigations have been performed on nanostructured ITO films deposited on ITO-coated commercial substrates in comparison to bare substrates. The physical microstructures have been investigated by grazing-incident X-ray diffraction (GIXRD), field-emission scanning electron microscopy (FE-SEM), and high-resolution transmission electron microscopy (HR-TEM). The electrical, optical, and hydrophobic properties were characterized by four-point probe measurements, UV–Vis–NIR spectrophotometry with angle-dependent technique, and contact angle goniometry, respectively. The results indicated that physical morphologies and nanorod diameters of ITO nanorod films were heavily influenced, and thus could be controlled, by deposition rate. The primary reason was self-annealing effect which occurred during film deposition and was crucial factor towards surface diffusion and film crystallinity. From the optical examinations, ITO nanorods deposited on the ITO-coated glasses exhibited significant improvements on transparent conductive oxide (TCO) properties from reference samples. The proposed ITO materials could therefore function as omnidirectional anti-reflection materials and super hydrophobic surface. This work have also proved that the ITO nanorods prepared by the electron-beam evaporation with the GLAD technique was highly promising for solar cell and optoelectronic applications.

1. Introduction

In the past decades, indium tin oxide (ITO) films were widely used as a transparent conducting oxide (TCO) layer for a variety of practical applications such as contact layers for solar cells [1–3], flat panel displays [4,5], and light-emitting devices [6,7]. The ITO films were extensively studied because of its highly degenerate n-type semiconductor with a wide band gap (3.5–4.3 eV), high transmittance in the visible region and high reflectance in infrared region, low resistivity, and long-term stability [8–10]. The nanostructured transparent conductors from the ITO nanorod films have recently attracted much attention due to large surface-to-volume ratios, low reflective index, enhanced antireflection, high

* Corresponding author.
** Corresponding author.
E-mail addresses: mati.horprathum@nectec.or.th (M. Horprathum), narong_kmutt@hotmail.com (N. Mungkung).

http://dx.doi.org/10.1016/j.cap.2016.11.018
1567-1739/

optical absorption due to randomly diffused light. In addition, enhanced formation of the ITO nanorod films would serve many potential applications, i.e., sensor devices [11,12], Bragg reflection filters [13], and improved efficiency of solar cells and optoelectronic devices [14–16]. Moreover, the roughened structures from the nanorod surface may enhance the hydrophobic property on the surface of TCO substrates which have a self-cleaning performance from water droplets. However, in order to prepare the ITO nanostructures to be utilized as the TCO with the omnidirectional antireflective and super-hydrophobic surfaces, the morphologies of the nanostructures must be well-controlled.

Various methods have been developed to fabricate the ITO nanorods, including sputtering [17–19], pulsed laser deposition [20–22], and molecular beam expitaxy [23,24]. From these methods, the nanostructures were grown at high substrate temperature (<500 °C) that yielded the nanostructures with random sizes, distributions, and orientations. Therefore, they were not reliable for commercial applications because of poor reproducibility. In addition, fabricating such large arrays of nanostructures poses a challenge even with the best developed nanofabrication methods by the top-down approach, i.e., the electron-beam lithography, nano-lithography, reactive ion etching and template-growth techniques, which suffer from low throughput, limited feature size and the need of expensive instrumentations. As an alternative approach, physical vapor deposition (PVD) method with an integrated glancing-angle deposition (GLAD) technique provides a vaporized particle flux arriving at the substrate from an oblique angle of incident. With the self-shadowing effect, limited adatom mobility, and finely controlled substrate motion, this approach would provide a variety of unique nanostructures, i.e., nanorods, nanoblades and zigzag nanocolumns [25–32]. Although the PVD with the GLAD technique suffered from the major limitation, especially from the large-area and low-cost deposition process, it offered the most promising commercialization to fabricate unique three-dimensional (3-D) nanostructures without lithographic process, i.e., surface-enhanced Raman substrates, nano-sensor devices, anti-reflection coatings on photovoltaic devices.

Studies of the ITO nanorod films formed by the electron-beam evaporation with the GLAD technique were focused on the structures, morphologies, electrical, optical, and hydrophobic properties based on the three-dimensional nanostructured films. There have been few research studies of the ITO nanorods fabricated by this technique because of a difficulty to control ternary compositions and limited adatom diffusions [33–36]. The ion-assisted reactive evaporation was an approach to control films compositions by supplying sufficient energy to oxygen ions during film growth.

In this study, we therefore explored the ion-assisted electron-beam evaporation with the GLAD technique in order to fabricate the nanostructured ITO films. In order to control the film crystallinity, the physical morphologies, the optical properties, and other performances, the influence of deposition rates to prepare the ITO nanorod films was investigated. The effects on structural, morphological, optical, electrical, and hydrophobic properties were extensively discussed.

2. Experimental details

The ITO nanorod films were prepared by an ion-assisted electron-beam evaporation (DENTON-DVB SJ-26C) with the GLAD technique, as shown in Fig. 1(a). In this study, the source materials were ITO (99.99%-purity) pellets with a composition of 90 wt% In_2O_3 and 10 wt% SnO_2 from K.J. Lesker. Two types of substrates, i.e.,

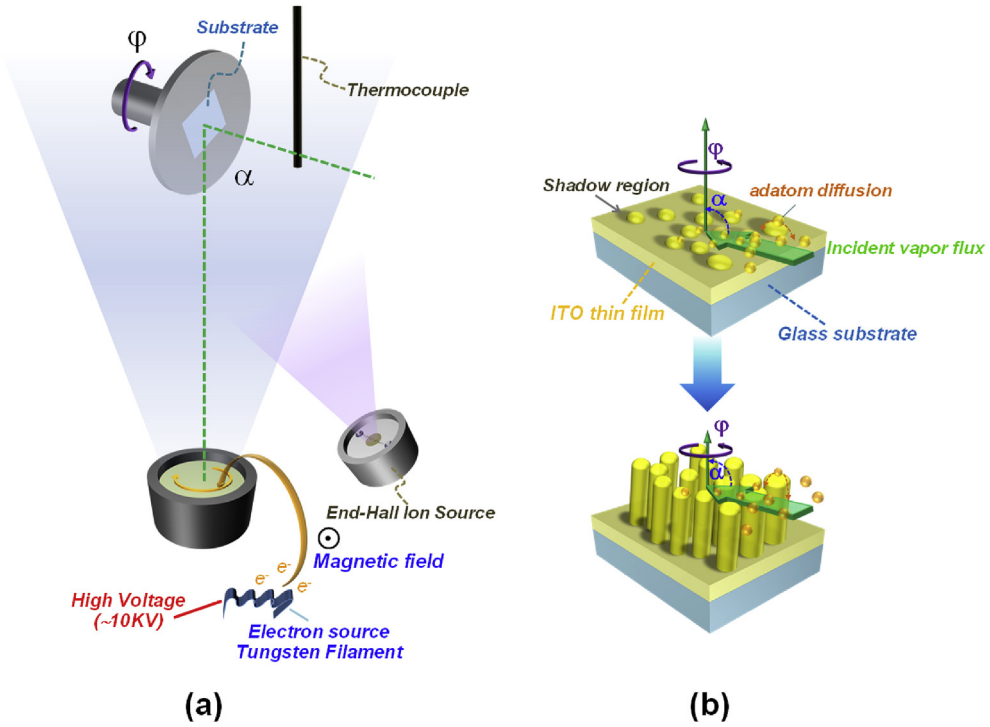

Fig. 1. Schematic illustrations of (a) the ITO nanorod films array fabricated by the ion-assisted electron beam evaporation with the GLAD technique and (b) the growths of the ITO nanorod films by the GLAD technique.

silicon (100) wafers and ITO-coated glass substrates (12Ω/□), had been ultrasonically cleaned in acetone, isopropanol, and deionized (DI) water, each for 10 min. The substrates were then dried with N_2 gas, and finally loaded into the deposition chamber. Prior to the thin-film deposition, the substrates were cleaned in an argon plasma at 13 sccm for 5 min with an end-Hall ion source in order to further remove surface contaminations. The deposition chamber attained a vacuum state by a mechanical pump (ALCATEL) and a cryogenic pump (ULVAC) with a base pressure of 8.0×10^{-7} Torr. Oxygen gas was introduced into the chamber at 8 sccm, controlled by a mass flow controller (MKS) via the end-Hall ion source in order to produced low energy oxygen ions. The ion source was operated at anion gun voltage and a current at 120 V and 1.0 A, respectively. During the film deposition, the electron gun voltage was 8.2 kV and the current were 0.3–0.8 mA, maintained at the operating pressure of 1.0×10^{-5} Torr. The substrate holder, which were mounted at a distance of 55 cm from the evaporation source, was fixed at an incident angle of 85° with respect to the surface normal and rotated at a speed of 30 rpm. The nanostructured ITO films were grown at different deposition rate from 0.1 to 0.75 nm/s and the thickness were maintained at 500 nm as monitored by a quartz-crystal monitor.

The crystallinity of the ITO nanorod films was characterized by using grazing-incidence X-ray diffraction (GIXRD, Rigaku TTRAX III). The Cu-K radiation was operated at 50 kV, 300 mA with a scanning speed of 2° per min at a step of 0.02° and a grazing incidence angle fixed at 0.4°. The morphologies of the ITO nanorods were investigated with high-resolution transmission electron microscopy (HRTEM, JEOL JEM-2010) performed with an acceleration voltage of 200 kV, and field-emission scanning electron microscopy (FE-SEM, Hitachi S-5200) performed with an operating voltage of 5 kV. The electrical properties of the prepared nanorod films were examined from the sheet resistance as measure by the four-point probe (Jandel RM3). The optical characteristics of the prepared nanorod films were further analyzed from optical transmission spectra as measured by UV-Vis-NIR spectrophotometry (Agilent, Cary 7000). The measurements were performed at a normal incident angle and a full spectral range of 200–2000 nm. By rotating the specimen, angle-dependent transmission measurements, with incidence angle defined relative to the surface normal of the samples, were also investigated. Finally, the super-hydrophobicity of the samples were examined from the water contact angle, as observed from a contact-angle goniometer.

3. Results and discussion

Fig. 2(a) shows XRD patterns of the ITO nanorod films deposited on silicon wafer substrates at different deposition rates. From the figure, we clearly observed that the ITO nanorod film prepared at the low deposition rate exhibited several sharp XRD peaks, indicating polycrystallinity with a cubic bixbyite structure. When the deposition rates were further increased, the crystallinity was instead decreased at all plane orientations towards amorphousness. This behavior could be explained that, usually, as-deposited GLAD samples without an external heating were amorphous because of shadowing effects and limited adatom diffusion. Both mechanisms inhibit the diffusivity of deposited atoms at room temperature [25,26]. In this work, the enhancement of the crystallinity occurred at the small deposition rate, which caused a longer deposition time. Based on the surface mobility, the longer deposition time would introduce the localized heating treatment of the substrate surface, and was therefore responsible for the higher

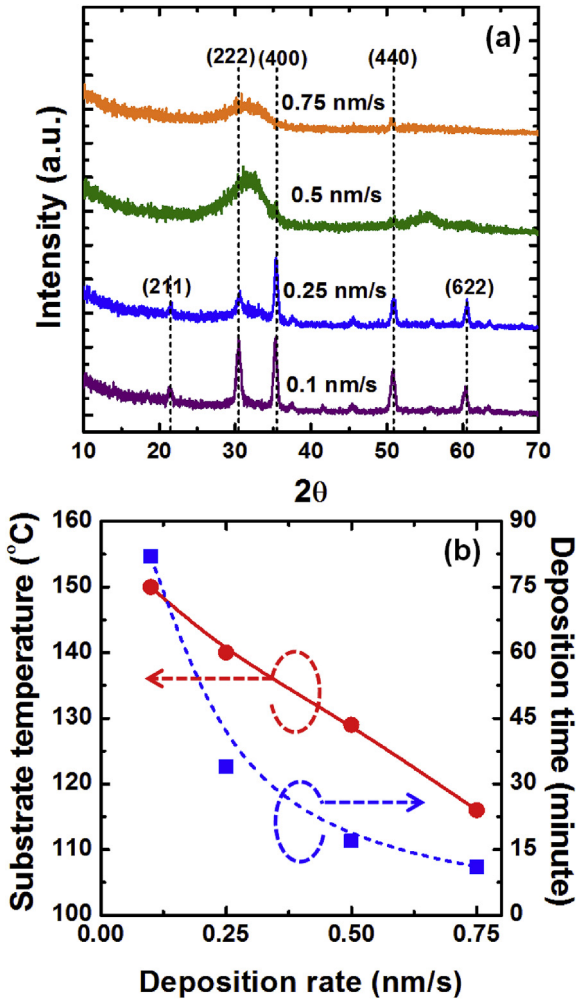

Fig. 2. (a) GIXRD patterns of the ITO nanorods films and (b) an evolution of the substrate temperature during the ITO nanorods grown by the GLAD technique at the different deposition rates.

adatom mobility. Note that, the XRD patterns representing the silicon substrates could not be observed from the GIXRD measurements because the grazing-incidence angle was fixed at 0.4°. During the measurements, the incident angle was slightly above the critical angle for the total reflection of the film materials, from which the XRD data would only represented the nanostructured ITO layer without those from the silicon substrates. To further investigate, an ambient temperature within the deposition chamber according to the substrate heating was measured by a thermocouple. Fig. 2(b) shows the evolution of the measured substrate temperature during the film deposition. From the figure, the film prepared at the low deposition rate clearly experienced the self-annealing treatment because of the longer deposition time.

The physical morphologies of the ITO nanorods prepared on the silicon wafers were examined, as shown in the FE-SEM images in Fig. 3. With the GLAD technique, the ITO nanorod films with partially isolated nanocolumnar structures were observed. The formations of the partially isolated nanocolumns occurred from both GLAD mechanisms, i.e., the atomic self-shadowing effects and the limited adatom diffusion, as schematically illustrated in Fig. 1(b). In this work, the FE-SEM images showed the ITO nanorod

films prepared at the different deposition rates, which played a major role towards the morphologies of the ITO nanorod films. At the small deposition rates, the ITO nanorods became large in the diameters and well-separated nanocolumns, as shown in Fig. 3, as caused by the self-annealing effect. From the circle insets in Fig. 3(a) and (b), the increase in the deposition time led to merged nanostructures, with varying nanorod diameters in the range of 80–92 nm, developed from a single columnar that existed in the beginning of the film growth. When the deposition rate was larger than 0.5 nm/s, the nanocolumnars without the structural broadening and merging were observed. From Fig. 3(c) and (d), no significant merged structures could be observed. This could be explained from the surface diffusion effect, where the decreased deposition rate caused longer deposition time, and eventually caused the increased ambient temperature that enhanced the adatom mobility. The overall phenomenon allowed the incoming particles the possibility to travel, but not at long distances, along the side of already existing columnar, thus gradually increasing the rods diameter [37]. For further comparison, Fig. 4 shows the FE-SEM images of the vertically align ITO nanorods grown on the ITO-coated glass substrates (ITO NRs/ITO-TF/Glass). The results indicated that the physical morphologies of the ITO NRs/ITO-TF/Glass were nearly identical to those of the ITO NRs/Si samples. From close inspections, the shapes, the sizes, and the porosity of the

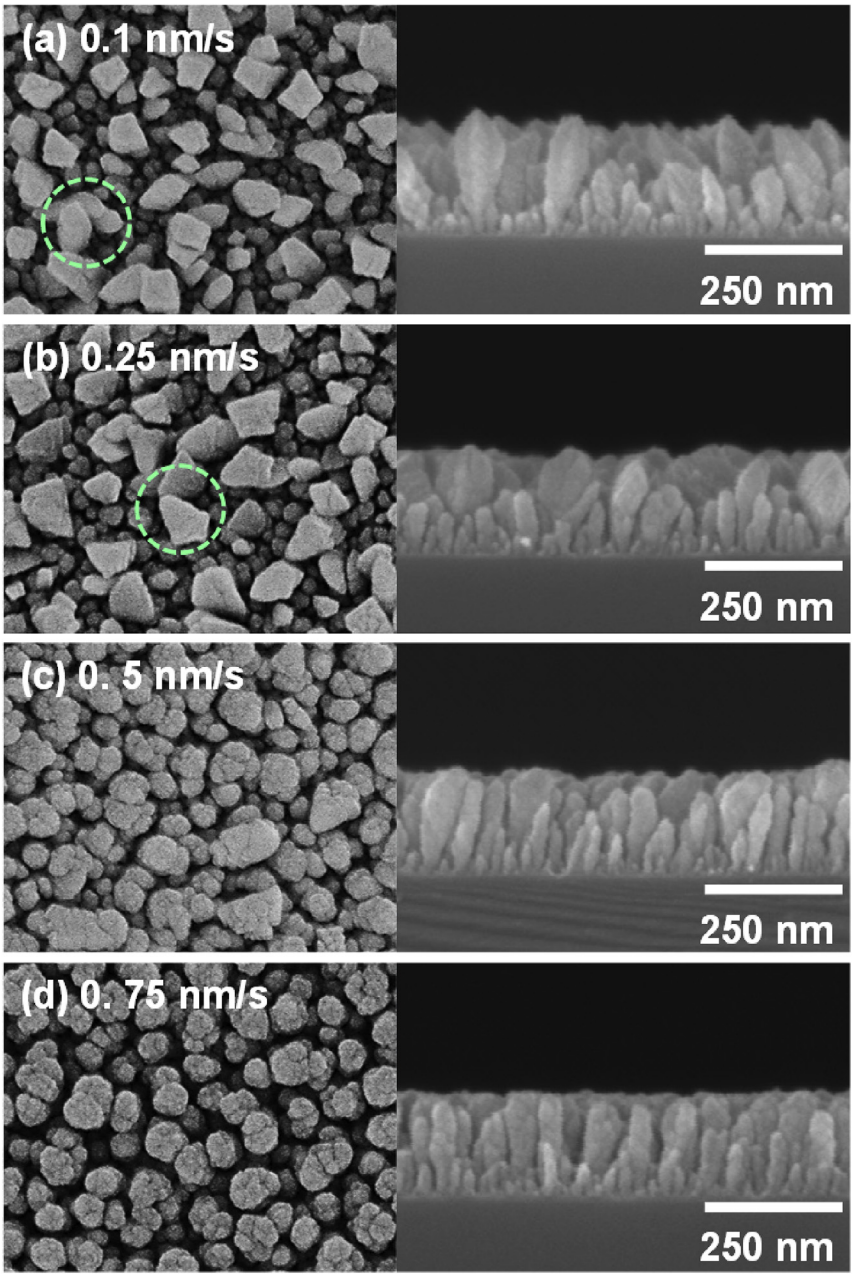

Fig. 3. Top-view and cross-sectional FE-SEM images of the ITO nanorod films on the Si substrate prepared by the GLAD technique at the different deposition rates.

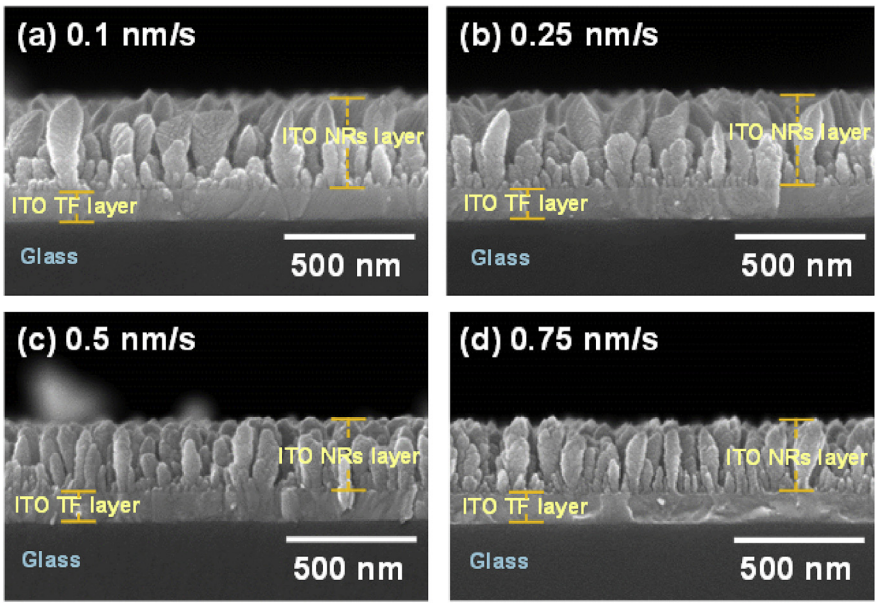

Fig. 4. Cross-sectional FE-SEM images of the ITO nanorod films on the commercial ITO thin film on the glass substrate prepared by the GLAD technique at the different deposition rates.

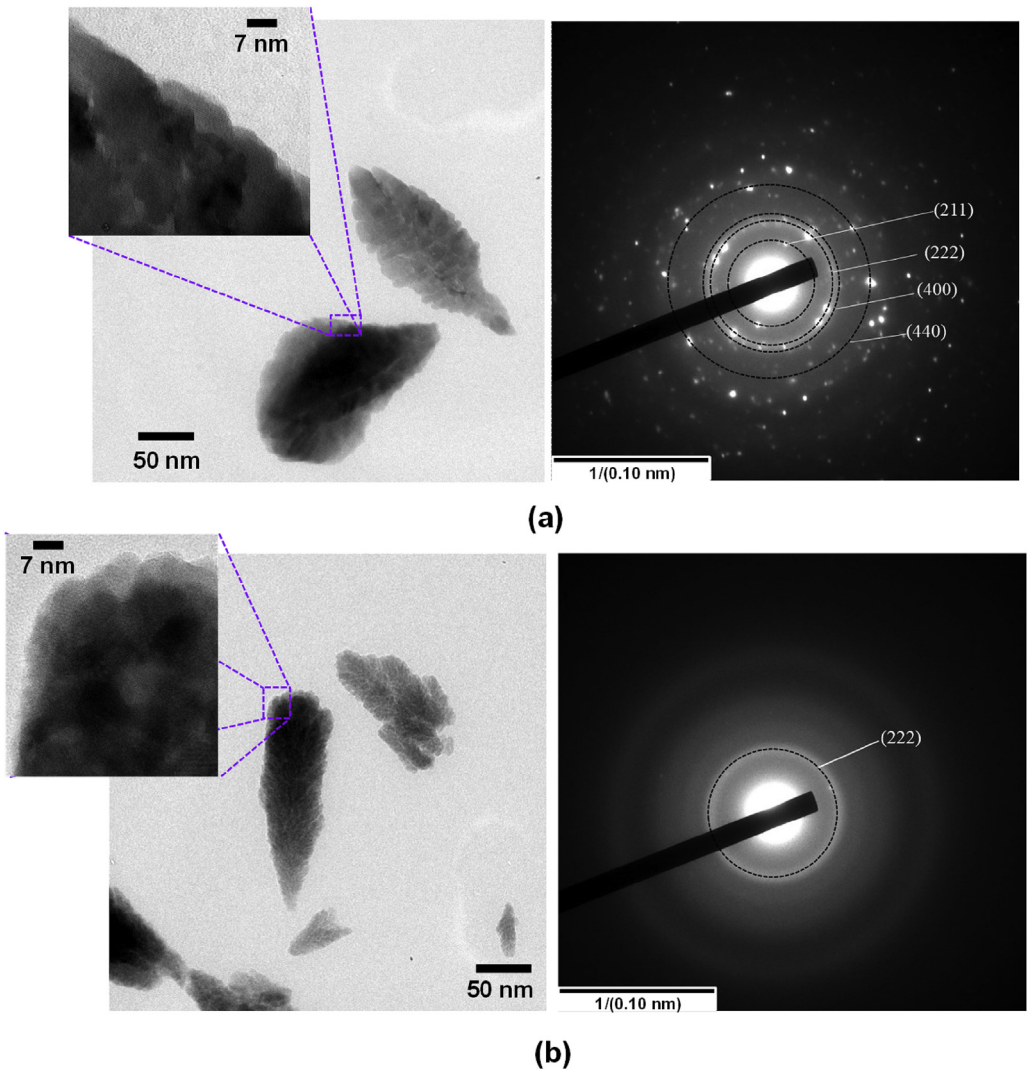

Fig. 5. HRTEM images of the single ITO nanorods taken from the samples prepared at (a) 0.1 and (b) 0.75 nm/s deposition rates.

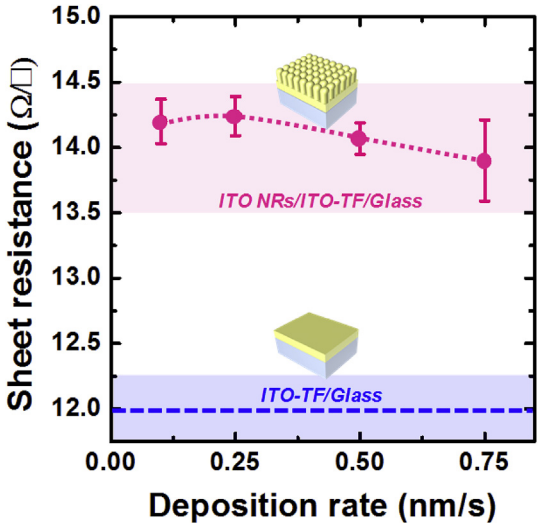

Fig. 6. Sheet resistance of the commercial ITO thin film on the glass and the ITO nanorod films deposited on the ITO-coated glass substrates at the different deposition rates.

ITO NRs on both types of the substrates were similar, while the lengths were different at approximately 50 nm. The primary reason was because the surface roughness of both types of the substrates were not significantly different, and they were small enough not to induce additional surface shadowing mechanisms and surface correlation that would promote the appearance of different structures. Further investigations of the individual ITO nanorods were performed with the high-resolution transmission electron microscopy (HRTEM). Fig. 5 shows the HRTEM images of the single ITO nanorods taken from the samples prepared at 0.1 and 0.75 nm/s. The figure clearly showed that only the individual ITO nanorod deposited at the smallest deposition rate had high crystallinity with the cubic bixbyite structure, as confirmed by the SAED patterns. The two inter-plane distances were measured, and the lattice planes could be indexed to ITO (211), (222), (400) and (440) as shown in Fig. 5(a).

To investigate the potentials of the ITO nanorod films to improve the TCO layer with antireflective properties, the sheet resistance, the optical transmission, and super-hydrophobic property of the ITO nanorod films were examined. In this studies, we compared the results from the ITO nanorod films deposited on the ITO-coated glass substrates (ITO NRs/ITO-TF/Glass) with the reference sample, i.e., the commercially available 120 nm-thick ITO thin film deposited on glass (ITO-TF/Glass). As shown in Fig. 6, the electrical analyses of the ITO NRs/ITO-TF/Glass were characterized by means of the four-point probe measurements. From the results, when the ITO nanorods were prepared at the increased deposition rate, the sheet resistance of the samples was slightly decreased. However, the results also indicated that the sheet resistance for all the samples was higher than the commercial ITO-TF/glass samples. The increased values of the sheet resistance occurred because of the increase in the porosity within the ITO nanostructures that would lead to the surface recombination loss [38, 39]. Note that, for the ITO nanorod films deposited at 0.1 nm/s, the resistivity was slightly decreased because of the relatively reduced gaps between each nanocolumnar. The overall results therefore indicated that all ITO nanorod films were acceptable to perform as the transparent conductive oxides for optoelectronic and solar cell applications.

Fig. 7(a) and (b) show photographs and the transmission spectra of the ITO NRs/ITO-TF/Glass deposited at various deposition rates in comparison with the commercial ITO-TF/Glass. It could be clearly observed that the ITO NRs/ITO-TF/Glass were more transparent than the ITO-TF/Glass. From the optical transmission, the oscillations in the spectral curves were observed due to the constructive or destructive interference of incident light between the air/nanorod films, nanorod film/TCO and TCO film/glass interfaces. Most samples generally showed high transmission in the visible range (390–700 nm). The average transmission in the visible region (T_{av}) of the ITO NRs/ITO-TF/Glass (87–89%) indicated the influence on transmission of the ITO-TF/Glass (85%) due to the gradual change in the refractive index between air [40], ITO nanorod and ITO film on glass show in Fig. 7(c). In addition, the difference in T_{av} of the ITO NRs/ITO-TF/Glass occurred from the geometrical morphologies and the diameters of the ITO nanorod films. Fig. 7(d)-(f) illustrates of the omnidirectional characteristics of the prepared samples at 500, 600 and 700 nm, respectively. The measurements were carried out over a range of incidence angle from −80° to 80°. The results clearly showed that the samples with the ITO nanorod films had higher optical transmission than the ITO-TF/Glass reference at all incidence angles. The results could demonstrated the performance of the prepared samples as the sensitivity to the incident angle due to the Fresnel reflections from the rear sides. The results also indicated that the ITO nanorod arrays were suitable for use as the antireflection layer, which would allow the high amount of the incident light into the solar cells.

Super-hydrophobic surface was also a promising characteristic for the self-cleaning omnidirectional TCO materials. Similar to the antireflection properties which strongly depended on the morphologies of the ITO nanorods, the self-cleaning properties was also dominated by the surface morphologies of the nanorod structures. Fig. 8 shows the static water contact angles with photographs of the water droplets on the surface of the ITO NRs/ITO-TF/Glass samples in comparison with the ITO-TF/Glass reference. From the figure, the ITO-TF/Glass reference sample had small water contact angle of 88.5°, while the ITO NRs/ITO-TF/Glass samples exhibited super-hydrophobicity in the range of (119–124°). These results also confirmed that the surface morphologies of the ITO films could help change from the Wenzel to Cassie–Baxter state as the ITO nanorod structures were deposited on the ITO-TF/Glass substrates. Therefore, the ITO nanorod films were expected to perform well in the self-cleaning activities.

4. Conclusion

We have presented the growth of the nanostructured ITO films by the ion-assisted electron-beam evaporation with the GLAD technique. We investigated the influences of the deposition rates of the ITO nanorods on the physical morphologies, the optical properties, and practical performances. The ITO nanostuctures prepared at 0.1 and 0.25 nm/s clearly indicated highly crystalline orientations on the merged nanostructures with large nanorod diameters because of the self-annealing effects. When the deposition rates were increased, the nanostructured ITO films became amorphous as observed from well-separated nanocolumns with the smaller nanorod diameters. The electrical properties and the optical transmission were also studied. The sheet resistances of the nanostructured ITO samples were only slightly increased in comparison with the commercial ITO-TF/glass substrates. The average transmission of the nanostructured ITO film/ITO-TF/glass samples were higher than the commercial reference sample over the visible wavelength range at all incident angles. In this study, we demonstrated the ITO nanorod samples with the average transmission of 87–89%, based on the transition in the refractive index profile from air to the ITO films that improved the AR characteristics. The study therefore demonstrated a simple, low-temperature processes to prepare the nanostructured ITO films based on the evaporation

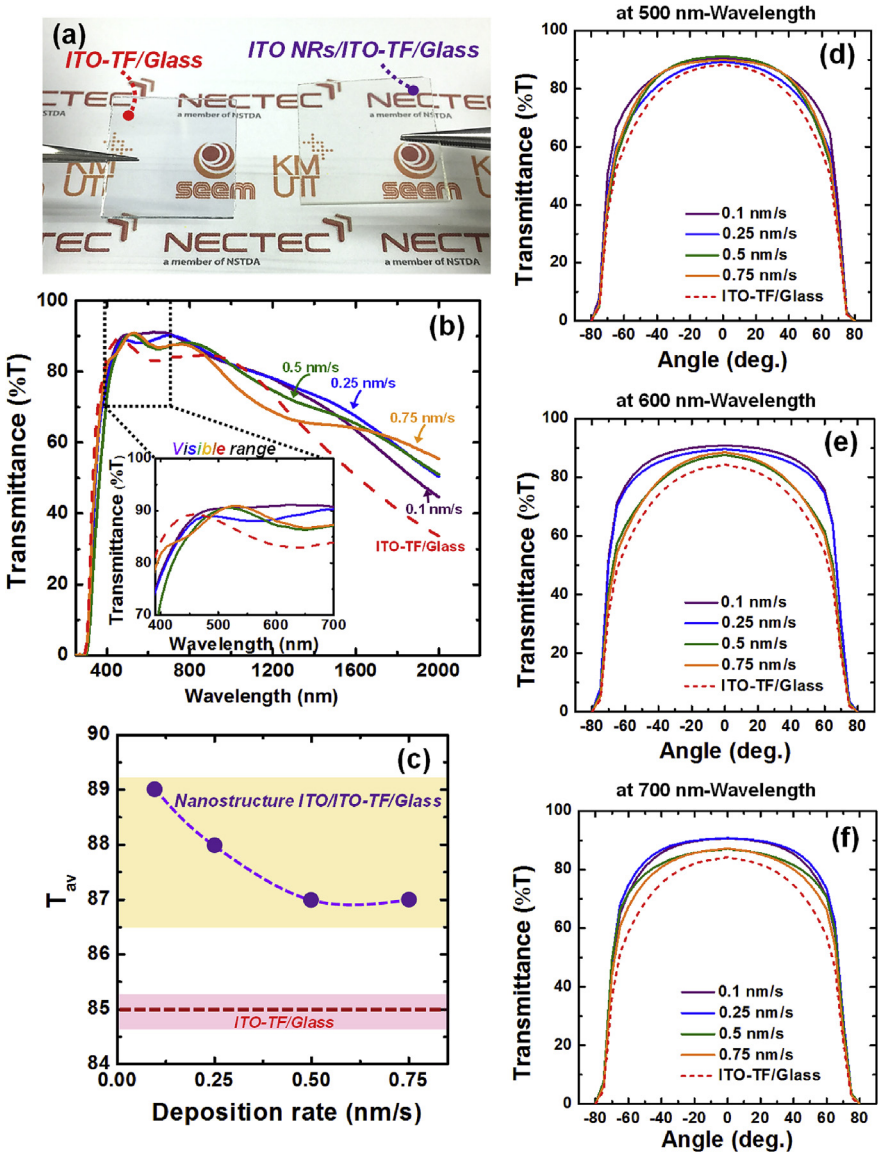

Fig. 7. Optical properties of the ITO nanorod films: (a) photographs of the commercial ITO thin film on glass and the ITO nanorod films deposited on the ITO-coated glass substrates, (b) the transmittance spectra of the ITO nanorods films, (c) the average transmission in the visible region (T_{av}) of the ITO nanorods films, and (e)–(f) the omnidirectional characteristics of the prepared samples at 500, 600 and 700 nm, respectively.

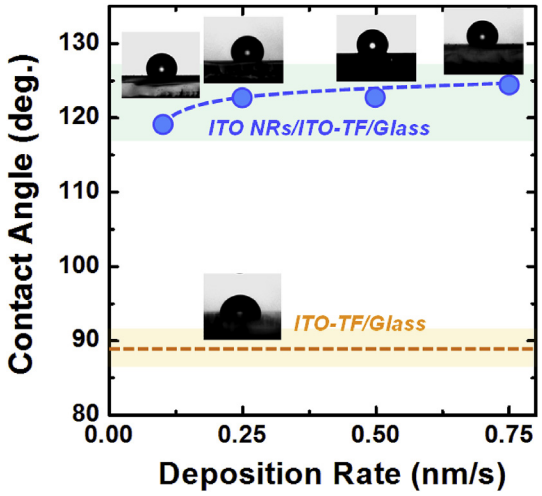

Fig. 8. Water contact angle of the commercial ITO thin film on the glass and the ITO nanorod films deposited on the ITO-coated glass substrates at various deposition rates.

with the GLAD technique. The well-controlled deposition rates would help improve the TCO performance for various applications in the optoelectronic and solar-cell applications.

Acknowledgment

This work was supported by School of Energy, Environment and Materials, King Mongkut's University of Technology Thonburi (KMUTT), Thailand, Faculty of Liberal-arts, Rajamangala University of Technology Rattanakosin, Thailand, and National Science and Technology Development Agency, Thailand. The authors gratefully acknowledge Optical Thin-Film Technology Laboratory (OTL), National Electronics and Computer Technology Center (NECTEC) for instrumentation and financial supports.

References

[1] J. Hotovy, J. Hüpkes, W. Böttler, E. Marins, L. Spiess, T. Kups, V. Smirnov, I. Hotovy, J. Kováč, Sputtered ITO for application in thin-film silicon solar cells: relationship between structural and electrical properties, Appl. Surf. Sci. 269 (2013) 81–87.

[2] J. Du, X.-L. Chen, C.-C. Liu, J. Ni, G.-F. Hou, Y. Zhao, X.-D. Zhang, Highly

transparent and conductive indium tin oxide thin films for solar cells grown by reactive thermal evaporation at low temperature, Appl. Phys. A 117 (2014) 815–822.
[3] A. Valla, P. Carroy, F. Ozanne, D. Muñoz, Understanding the role of mobility of ITO films for silicon heterojunction solar cell applications, Sol. Energy Mat. Sol. Cells 157 (2016) 874–880.
[4] B.H. Lee, L.G. Kim, S.W. Cho, S.H. Lee, Effect of process parameters on the characteristics of indium tin oxide thin film for flat panel display application, Thin Solid Films 302 (1997) 25–30.
[5] S.K. Park, J. In Han, W.K. Kim, M. GiKwak, Deposition of indium–tin-oxide films on polymer substrates for application in plastic-based flat panel displays, Thin Solid Films 397 (2001) 49–55.
[6] Y. Gil, H. Kim, Hybrid ITO transparent conductive electrodes embedded with Pt nanoclusters for enhanced output efficiency of GaN-based light-emitting diodes, Thin Solid Films 603 (2016) 307–312.
[7] W. Wang, H. Peng, S. Chen, Highly transparent quantum-dot light-emitting diodes with sputtered indium-tin-oxide electrodes, J. Mater. Chem. C 4 (2016) 1838–1841.
[8] D. Raoufi, A. Kiasatpour, H.R. Fallah, A.S.H. Rosatian, Surface characterization and microstructure of ITO thin films at different annealing temperatures, Appl. Surf. Sci. 253 (2007) 9085–9090.
[9] H. Kim, A. Pique, J.S. Horwitz, H. Mattoussi, H. Murata, Z.H. Kafafi, D.B. Chrisey, Indium tin oxide thin films for organic light-emitting devices, Appl. Phys. Lett. 74 (1999) 3444.
[10] H.J. Kim, J.W. Bae, J.S. Kim, K.S. Kim, Y.C. Jang, G.Y. Yeom, N.-E. Lee, Electrical, optical, and structural characteristics of ITO thin films by krypton and oxygen dual ion-beam assisted evaporation at room temperature, Thin Solid Films 377–378 (2000) 115–121.
[11] S. Xu, Y. Shi, Low temperature high sensor response nano gas sensor using ITO nanofibers, Sens. Actuators B Chem. 143 (2009) 71–75.
[12] X. Li, G.M. Kale, Influence of thickness of ITO sensing electrode film on sensing performance of planar mixed potential CO sensor, Sens. Actuators B Chem. 120 (2006) 150–155.
[13] M.F. Schubert, J.-Q. Xi, J.K. Kim, E.F. Schubert, Distributed Bragg reflector consisting of high- and low-refractive-index thin film layers made of the same material, Appl. Phys. Lett. 90 (2007) 141115.
[14] Y.-C. Chao, F.-M. Zhan, H.-D. Li, Indium-tin-oxide nanorods for efficient light trapping in polymer solar cells, RSC Adv. 4 (2014) 30881–30886.
[15] H.-Y. Lee, H.-L. Huang, O.P. Pchelyakov, N.A. Pakhanov, Performance improvement mechanisms of bias-assisted photoelectrochemical treated GaSb-based solar cells with ITO nanorod array, Prog. Photovolt. Res. Appl. 24 (2) (2016) 195–199.
[16] J. Gao, R. Chen, D.H. Li, L. Jiang, J.C. Ye, X.C. Ma, X.D. Chen, Q.H. Xiong, H.D. Sun, T. Wu, UV light emitting transparent conducting tin-doped indium oxide (ITO) nanowires, Nanotechnology 22 (2011) 195706.
[17] H. Kim, M.D. Kumar, M. Patel, J. Kim, ITO nanowires-embedding transparent NiO/ZnO photodetector, Mater. Res. Bull. 83 (2016) 35–40.
[18] G.O. Setti, M.B. Mamián-López, P.R. Pessoa, R.J. Poppi, E. Joanni, D.P. Jesus, Sputtered gold-coated ITO nanowires by alternating depositions from Indium and ITO targets for application in surface-enhanced Raman scattering, Appl. Surf. Sci. 347 (2015) 17–22.
[19] M.K. Fung, Y.C. Sun, A.M.C. Ng, X.Y. Chen, K.K. Wong, A.B. Djurisic, W.K. Chan, Indium tin oxide nanowires growth by dc sputtering, Appl. Phys. A Mater 104 (2011) 1075–1080.
[20] G. Meng, T. Yanagida, H. Yoshida, K. Nagashima, M. Kanai, F. Zhuge, Y. He, A. Klamchuen, S. Rahong, X. Fang, S. Takeda, T. Kawai, A flux induced crystal phase transition in the vapor–liquid–solid growth of indium-tin oxide nanowires, Nanoscale 6 (2014) 7033–7038.
[21] G. Meng, T. Yanagida, K. Nagashima, H. Yoshida, M. Kanai, A. Klamchuen, F. Zhuge, Y. He, S. Rahong, X. Fang, S. Takeda, T. Kawai, Impact of Preferential indium nucleation on electrical conductivity of vapor–liquid–solid grown indium–tin oxide nanowires, J. Am. Chem. Soc. 135 (2013) 7033–7038.
[22] A. Klamchuen, H. Tanaka, D. Tanaka, H. Toyama, G. Meng, S. Rahong, K. Nagashima, M. Kanai, T. Yanagida, T. Kawai, T. Ogawa, Advanced photo-assisted atomic switches produced using ITO nanowire electrodes and molten photoconductive organic semiconductors, Adv. Mater. 25 (2013) 5893–5897.
[23] C. O'Dwyer, C.M. Sotomayor Torres, Epitaxial growth of an antireflective, conductive, graded index ITO nanowire layer, Front. Phys. 1 (18) (2013) 1–8.
[24] C. O'Dwyer, M. Szachowicz, G. Visimberga, V. Lavayen, S.B. Newcomb, C.M. Sotomayor Torres, Bottom-up growth of fully transparent contact layers of indium tin oxide nanowires for light-emitting devices, Nat. Nanotechnol. 4 (2009) 239–244.
[25] K. Robbie, M.J. Brett, Sculptured thin films and glancing angle deposition: growth mechanics and applications (May/June (3)), J. Vac. Sci. Technol. A 15 (1997).
[26] Y.P. Zhao, D.X. Ye, G.C. Wang, T.M. Lu, Designing nanostructures by glancing angle deposition, Proc. SPIE 5219 (2003) 59–73.
[27] D. Deniz, D.J. Frankel, R.J. Lad, Nanostructured tungsten and tungsten trioxide films prepared by glancing angle deposition, Thin Solid Films 518 (2010) 4095–4099.
[28] D. Deniz, R.J. Lad, Temperature threshold for nanorod structuring of metal and oxide films grown by glancing angle deposition, J. Vac. Sci. Technol. A 29 (2011) 011020.
[29] H. Tanaka, P.S. Weiss, M.W. Horn, Fabrication of periodic standing rod arrays by the shadow cone method (December (6)), Int. J. Nanosci. 5 (2006).
[30] M. Horprathum, T. Srichaiyaperk, B. Samransuksamer, A. Wisitsoraat, P. Eiamchai, S. Limwichean, C. Chananonnawathorn, K. Aiempanakit, N. Nuntawong, V. Patthanasettakul, C. Oros, S. Porntheeraphat, P. Songsiriritthigul, H. Nakajima, A. Tuantranont, P. Chindaudom, Ultrasensitive hydrogen sensor based on Pt-decorated WO_3 nanorods prepared by glancing-angle dc magnetron sputtering, ACS Appl. Mater. Interfaces 6 (2014) 22051–22060.
[31] M. Horprathum, K. Limwichean, A. Wisitsoraat, P. Eiamchai, K. Aiempanakit, P. Limnonthakul, N. Nuntawong, V. Pattantsetakul, A. Tuantranont, P. Chindaudom, NO_2-sensing properties of WO_3 nanorods prepared by glancing gangle DC magnetron sputtering, Sens. Actuators B Chem. 176 (2013) 685–691.
[32] C. Oros, M. Horprathum, A. Wisitsoraat, T. Srichaiyaperk, B. Samransuksamer, S. Limwichean, P. Eiamchai, D. Phokharatkul, N. Nuntawong, C. Chananonnawathorn, V. Patthanasettakul, A. Klamchuen, J. Kaewkhao, A. Tuantranont, P. Chindaudom, Ultra-sensitive NO_2 sensor based on vertically aligned SnO_2 nanorods deposited by DC reactive magnetron sputtering with glancing angle deposition technique, Sens. Actuators B Chem. 223 (2016) 936–945.
[33] S.H. Lee, J.W. Leem, X.-Y. Guan, J.S. Yu, Highly-reflective and conductive distributed Bragg reflectors based on glancing angle deposited indium tin oxide thin films for silicon optoelectronic applications, Thin Solid Films 591 (Part B, 30) (September 2015) 351–356.
[34] J.W. Leem, J.S. Yu, Glancing angle deposited ITO films for efficiency enhancement of a-Si:H/μc-Si:H tandem thin film solar cells, Opt. Express 19 (2011) A258.
[35] A. Forget, R.T. Tucker, M.J. Brett, B. Limoges, V. Balland, Tuning the reactivity of nanostructured indium tin oxide electrodes toward chemisorption, Chem. Commun. 51 (2015) 6944.
[36] A.W. Sood, D.J. Poxson, F.W. Mont, S. Chhajed, J. Cho, E.F. Schubert, R.E. Welser, N.K. Dhar, A.K. Sood, Experimental and theoretical study of the optical and electrical properties of nanostructured indium tin oxide fabricated by oblique-angle deposition, J. Nanosci. Nanotechnol. 12 (2012) 3950–3953.
[37] C. Patzig, A. Miessler, T. Karabacak, B. Rauschenbach, Arbitrarily shaped Si nanostructures by glancing angle ion beam sputter deposition, Phys. Status Solidi B 247 (2010) 1310–1321.
[38] J.W. Leem, J.S. Yu, Indium tin oxide subwavelength nanostructures with surface antireflection and superhydrophilicity for high-efficiency Si-based thin film solar cells, Opt. Express. 20 (2012) A431.
[39] Y. Zhong, Y.C. Shin, C.M. Kim, B.G. Lee, E.H. Kim, Y.J. Park, K.M.A. Sobahan, C.K. Hwangbo, Y.P. Lee, T.G. Kim, Optical and electrical properties of indium tin oxide thin films with tilted and spiral microstructures prepared by oblique angle deposition, J. Mater. Res. 23 (2008) 2500–2505.
[40] S. Chhajed, M.F. Schubert, J.K. Kim, E.F. Schubert, Nanostructured multilayer graded-index antireflection coating for Si solar cells with broadband and omnidirectional characteristics, Appl. Phys. Lett. 93 (2008) 251108.